International Research Journal of Engineering and Technology (IRJET) e-ISSN: 2395-0056
Volume: 10 Issue: 05 | May 2023 www.irjet.net p-ISSN: 2395-0072

ANALYSIS OF THERMAL PERFORMANCE OF SOLAR COLLECTOR WITH LONGITUDINAL FINS

Abhilash Kumar Pandey[1] Asst. Prof. Shailendra Kumar Shukla[2]

[1]*Mtech Scholar, dept of mechanical Engineering, Rewa Institute of Technology, Rewa*
[2] Asst. Prof., *dept of mechanical engineering, Rewa Institute of Technology, Rewa*

Abstract-*The performance of solar collectors as a means of generating renewable energy is the primary emphasis of this work. To begin, a numerical simulation will be carried out and then contrasted with the results of previous studies in order to validate the findings that were achieved. There are a total of six unique collector models that have been created; three of these collector models feature various fins (2, 4, 6), while the remaining three collector models have varying fin heights The thermal and dynamic behavior of the air flow inside these various cases was analyzed for different values of solar radiation and for other different values of air velocity at the collector inlet. The values of solar radiation and air velocity were determined by measuring the amount of energy that was absorbed by the surface area of the collector. This report presents, analyzes, compares, and interprets in considerable depth the temperature contours, velocity fields, and temperature change at the collector outlet as functions of solar radiation and air velocity for each model. All of this was accomplished with the assistance of the ANSYS FLUENT calculation code, which was used to solve the conservation equations of mass, amount of motion, and energy by using the approach of finite volume.*

Keywords: *solar collectors, renewable energy, fins, solar radiation*

INTRODUCTION

Solar energy

Solar energy is a promising source of renewable energy that has gained significant attention in recent years due to its sustainability and environmental benefits. One of the key components of a solar thermal system is the solar collector, which absorbs solar radiation and converts it into heat that can be used for various applications such as space heating and hot water production. In order to improve the efficiency of solar collectors, researchers have been exploring various design modifications, including the use of longitudinal fins. Longitudinal fins are thin, elongated strips that are attached to the absorber plate of a solar collector. They increase the surface area of the absorber plate, which enhances heat transfer and improves thermal performance.

The use of longitudinal fins has been shown to increase the efficiency of solar collectors in a variety of applications. However, the optimal design and configuration of longitudinal fins depend on several factors, including the operating conditions of the solar collector and the materials used in the fins. Therefore, a detailed analysis of the thermal performance of solar collectors with longitudinal fins is necessary to identify the most effective design parameters for different applications. In this research paper, we present an analysis of the thermal performance of a solar collector with longitudinal fins. We investigate the effects of fin height, fin thickness, and fin spacing on the thermal efficiency of the collector under different operating conditions. We also examine the impact of the material properties of the fins on the overall performance of the solar collector.

METHODOLOGY

Physical model

The geometric configuration of the problem under study is shown schematically in Figure 3.1. The dimensions of the solar collector presented and used in this work are based on experimental data published by A. Dahmani et al [39]. It is a solar collector of 1.97m in length and 0.98m in width.

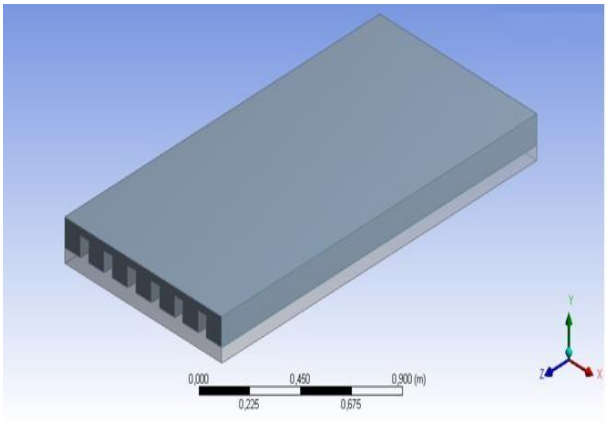

Figure 3. 1: General diagram of the physical domain

During this study, an interest is given to the study of the effect of system size on the dynamic and thermal behaviour of the fluid, for this, three heights and three numbers of different fins (Table 3.1) were examined and compared in detail. The dimensions and details that accompany each model are also presented in Table 3.2.

Simplifying assumptions

The formulation of the problem studied is based on a number of simplifying assumptions, hypotheses related to geometry, type of flow, transfer mechanisms and phase change problems. In order to allow a simple and realistic resolution", we considered the following assumptions:

- The fluid flow is assumed to be permanent and laminar.
- The viscous fluid is Newtonian and incompressible.

Conservation of mass

The equation for conservation of mass is:

$$\frac{\partial \rho}{\partial t} + \frac{d(\rho u)}{dx} + \frac{d(\rho v)}{dy} + \frac{d(\rho w)}{dz} = 0$$

Since the flow is permanent

$$\frac{\partial \rho}{\partial t} = 0$$

So the equation becomes:

$$\frac{d(\rho u)}{dx} + \frac{d(\rho v)}{dy} + \frac{d(\rho w)}{dz} = 0$$

Principles of CFD codes

CFD codes make it possible to solve numerically the "equations governing the motions of a fluid, i.e. the equations reflect the conservation of the mass and momentum of the fluid (Navier-Stokes equations), as well as the conservation of its enthalpy. There are a large number of CFD codes available, for our work, we have chosen the Fluent CFD code (Workbench version 14.0), the latter allows us to meet our calculation needs.

- To build a CFD model, there are several steps:
- The construction of geometry.
- The construction of the mesh.
- The selection of physical models: in fact, these are rarely the exact equations of

Part of geometry

We created the geometry with ANSYS Design Modeler software, which allows you to make 2D plots (Sketch), to create 3D objects from sketches (by extrusion etc...) and manipulate 3D objects.

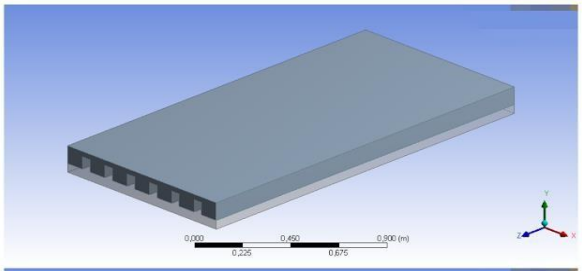

Figure 3. 3: The ANSYS Design Modeler software interface.

Mesh part

To create the mesh, we launched ANSYS Meshing by double-clicking on Mesh in the Workbench box. The choice of mesh is an essential step in digital simulation [45].

It is therefore important to choose a mesh that best adapts to the problems considered.

In this study, a uniform structured hexahedral mesh refined at the walls was chosen. The generated mesh results are presented in Table 3.3"

Table 3. 3: Details of the generated mesh.

Partitions	Nodes	Elements	Growth rate
1	31108	21600	1,2

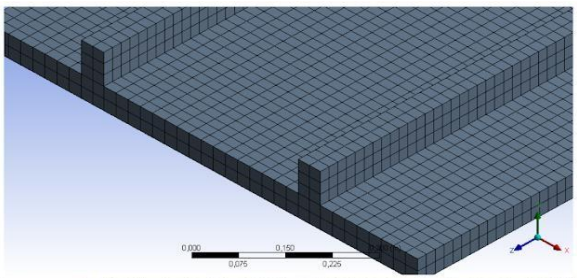

Figure 3. 4: The final generated mesh of the domain studied.

Choice of the two calculation methods Fluent of two calculation modes:

- **Double-precision mode:** In double-precision mode, floating-point numbers are represented using 64 bits.
- **Single-precision mode:** Single-precision mode uses a 32-bit representation.

The thermophysical properties of the materials used

Table 3.4: The thermo-physical properties of the materials used.

Material	Density	Specific heat	Thermal conductivity
Air	1.225	1006.43	0.0242
Aluminium	2719	871	202.4
Glass	2530	7205	0.93

Boundary conditions

Depending on the physical problem being addressed, the boundary conditions are different and their compatibility with numerical models is associated with a direct impact on the convergence and realism of the results of numerical simulations. Several types of boundary conditions are offered in CFDs".

In our case, to solve the system of equation obtained, it is necessary to introduce the following boundary conditions:

- **Input:** a uniform air velocity and temperature are imposed on the input of the calculation domain.
- **At the level of the absorber and the glazing:** A radiative flux of different solar intensities is applied.
- **Output:** At the exit of the calculation domain, an atmospheric pressure is applied as boundary conditions.

Table 3. 5: Type of boundary conditions programmed in Fluent.

Zone	Type
Absorber	Wall
Insulator	Wall
Glazing	Wall
Entrance	Velocity-inlet
Fluid domain	Interior
Solid domain	Interior
Exit	Pressure-outlet
Walls	Wall
Fins	Wall

Numerical diagrams

(a) Resolution of the speed-pressure coupling

The "Navier–Stokes equations consist of the mass conservation equation and the momentum conservation equations. Their resolution requires obtaining at all times, a coherent pressure field and a velocity field. Fast-pressure couplings tricky to deal with for incompressible flows because pressure does not appear explicitly in the mass conservation equation.

RESULTS AND DISCUSSION

Introduction

The governing equations are solved by the finite volume method using a Fluent calculation code. The velocity and temperature fields were obtained and presented for all the geometry considered at different heights and number of fins. The variation of the average velocity as well as the average temperature for all the cases studied is also presented in this chapter for different values of entry velocity and for different intensity of solar radiation.

Validation of the numerical model

Before starting the numerical simulation dealing with the influence of the various parameters, a comparison of the results of the present study with those obtained by Dahmani et al [39] was carried out under the conditions used in their experimental work carried out on a solar collector of simple form.

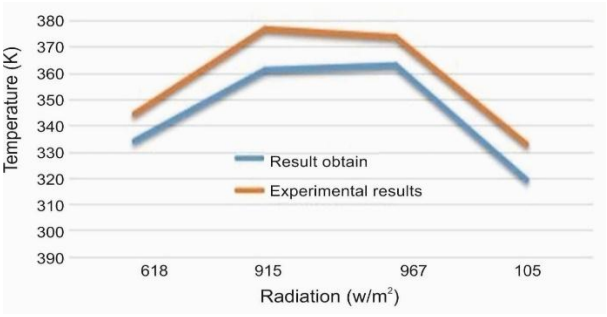

Figure 4. 1: Comparison of the evolution of the temperature at the outlet as a function of the solar radiation, with the results of Dahmani et al. [39]

Figures 4.1 represent the evolution of the air temperature at the collector outlet as a function of solar radiation obtained numerically by Fluent and experimentally by Dahmani et al. [39].

For the outlet temperature, it can be seen that the mean error of the results obtained with the experimental values [39] is of the order of 1.42%. Then the results obtained are very accurate compared to those of Dahmani et al. [39].

This comparison shows the good accuracy of our results compared to those proposed by Dahmani et al. [39] This may provide validation for the results developed below.

Influence of number of finned rows

For an air inlet velocity of 0.2 m/s, ambient temperature of 296 K and solar intensity of 618W/m2. Figures (4.2) and (4.3) illustrate respectively the temperature contours and velocity vectors of a flow relative to a solar vector1.98 m long and for different numbers of fins (2 ranges, 4 ranges and 6 ranges).

Temperature contour

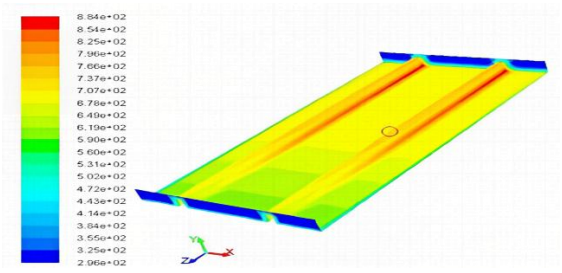

(a)

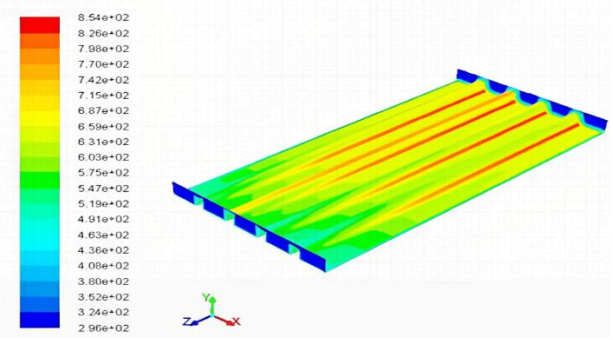

(b)

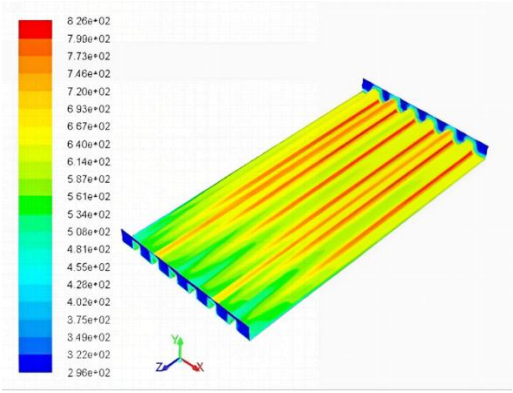

(c)

Figure 4. 2: Temperature contours for different number of fin rows for a solar intensity of 618 W/m2; a: 2 rows, b: 4 rows and c: 6 rows.

Figure 4.2 shows the heat distribution in the system along the collector "1.97m" and for different row numbers of fins 2, 4 and 6 respectively. The temperature fields shown in Figure 4.2 reflect the convective and dynamic structures of laminar flow. Indeed, it is clear that small temperature gradients are generated near the collector inlet, because fresh air of low temperature is always sucked in. However, the temperature began to rise more and more from 1/3 of the channel as it approached the outlet. This is due to the heat exchange between the absorber and the air.

Velocity fields

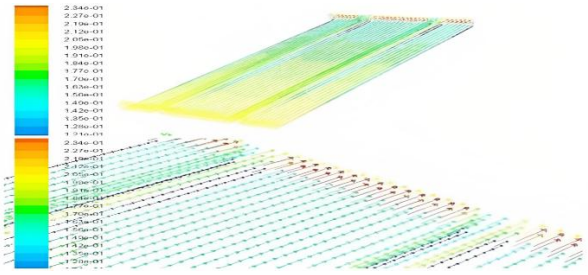

2 rows

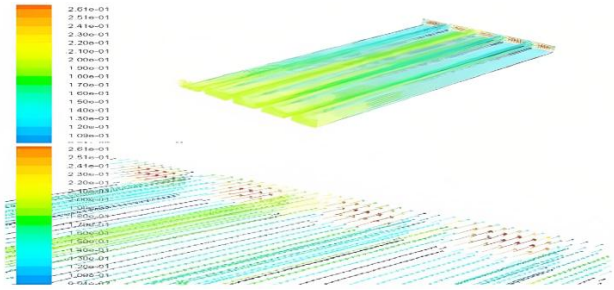

4 rows

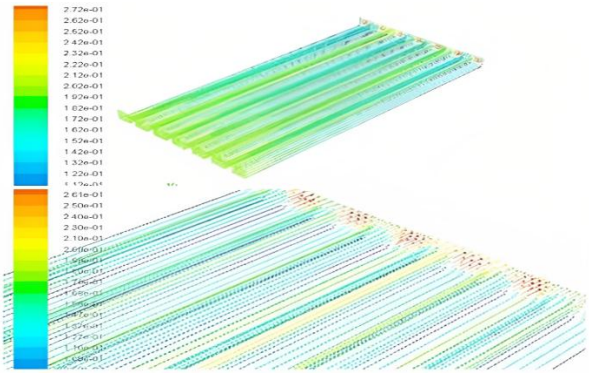

6 rows

Figure 4.3: Velocity vector field for different number of fin rows for a solar intensity of 618W/m2.

Figure 4.3 shows the velocity vector fields for different finning rows (2, 4 and 6 rows) at a solar intensity of 618 W/m2.

We notice that the fluid accelerates just upstream of the channel and it begins to decrease as it approaches the exit, this is explained by the friction with the walls of the collector and also with the fins, this friction generates in general the resistance to movement and consequently gives rise to a phenomenon of braking. The lowest velocity values are observed in the vicinity of the absorber-fin contact angle.

Table 4. 1: Comparison between the average air velocity at the outlet for the three numbers of rows.

Number of rows	Average air velocity at outlet (m/s)
2	0,2
4	0,2
6	0,2

According to figure 4.3 and table 4.1, the average velocity of the air outlet at the system level remains constant for all three cases. Because of flow conservation (Q input = Q_{output})

We know that there is a direct relationship between flow, area and speed Q = V.S

Ventured S input = V output S output (S input = S output V in $\Rightarrow$ = V_{output}).

Influence of fin height

The results shown in Figures 4.4 and 4.5 illustrate the evolution of the velocity fields and the temperature contour of a flow relative to a solar collector for different fin heights in a collector of length and width of 1.97m and 0.98m respectively and for a solar intensity of 618 W/m2.

Temperature contour

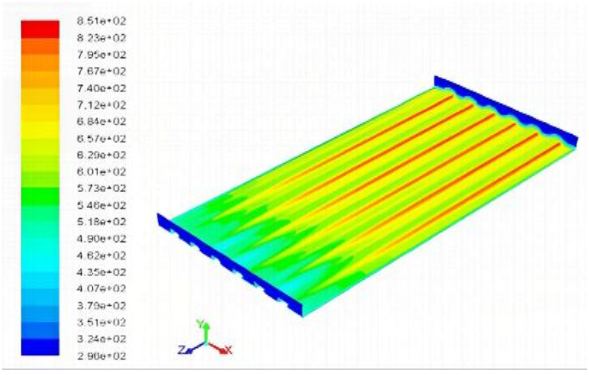

0.03m

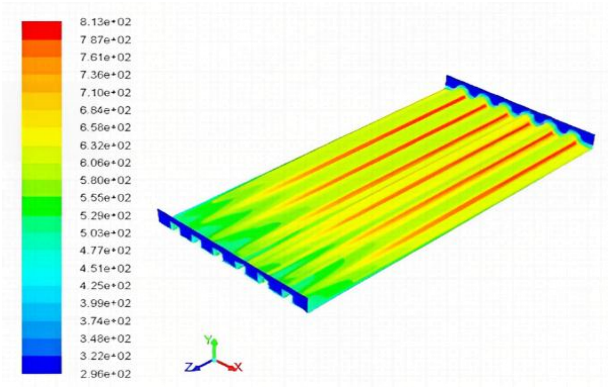

0.05m

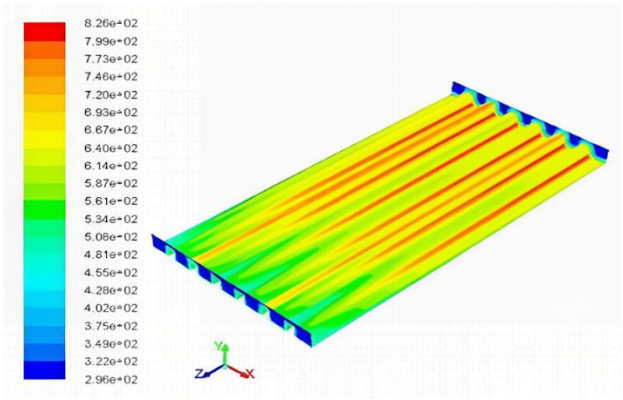

0.07m

Figure 4. 4: Temperature contours for different fin heights at a solar intensity of 618 W/m2.

Table 4. 2: Comparison between the average temperatures at the outlet for the three fin heights studied.

Fin-heights (m)	Average temperature at the exit (K)
0,03	518.68
0,05	527.23
0,07	534.78

Figure 4.4 shows the heat distribution in a system 1.98 m long and 0.98 m wide with six rows of fins of different heights: 0.03, 0.05 and 0.07 m. The mean temperature values at the collector output for the three different fin heights are shown in Table 4.2. The results show a significant temperature difference from one case to another, the case of the solar collector of 0.07m height of fins has a significant average temperature at the exit compared to the other two cases. Result shows a proportionality between the height of fins and the temperature at the outlet and this because of the increase in the catchment section which depends directly on the height of fins.

Velocity fields

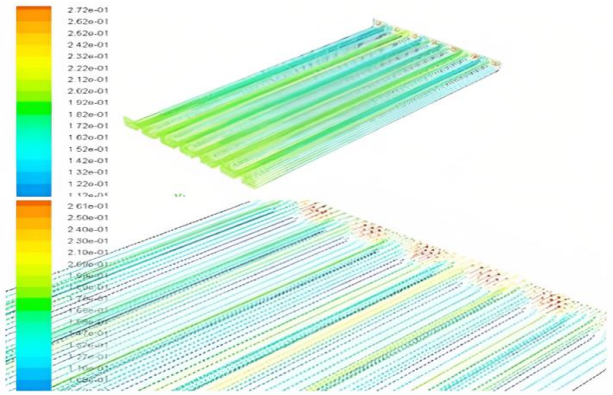

0.03m

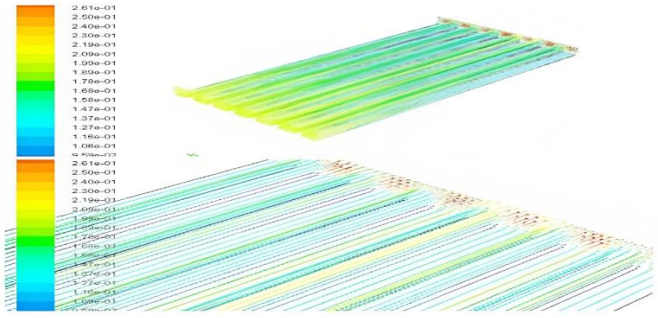

0.05m

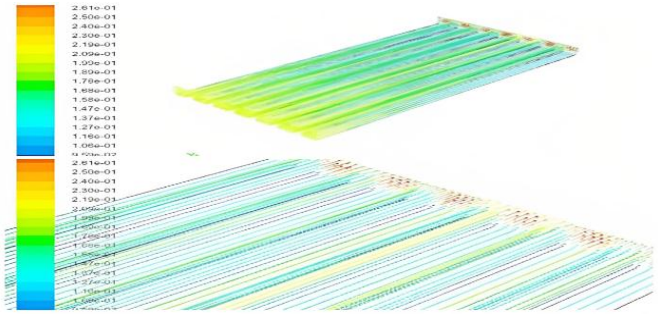

0.07m

Figure 4. 5: Velocity vector field for different height of collector fins at a solar intensity of 618 W/m2.

Figure 4.5 shows the velocity vector field for a solar collector with six rows of fins of different heights: 0.03, 0.05 and 0.07m. From the figures presented, it can be seen that there is no difference in velocity between the inlet and outlet in the stack for all three cases, a logical result because it confirms the principle of conservation of mass.

The velocity vector fields presented for the different cases show low velocities in the vicinity of walls, this is friction phenomena. The increase in fin height contributes to the increase in the exchange surface and therefore has a thermal advantage but on the other hand it is associated by additional pressure drops.

Evolution of the average temperature as a function of solar intensity

The results were taken for the following input parameters for each model:

- An input speed of 0.2 m/s.
- An ambient temperature of 298 K.

a. For the three different number of rows

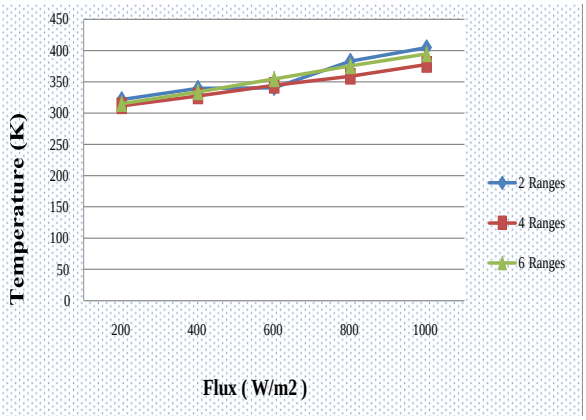

Figure 4. 6: Evolution of the average temperature at the collector output as a function of solar intensity for different rows of fins.

b. For the three different fin heights

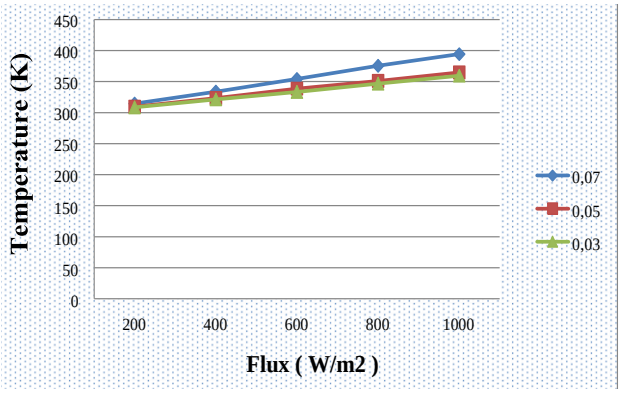

Figure 4. 7: Evolution of the average temperature at the output of the collector as a function of the solar intensity for the three different heights of fins.

Figures 4.6 and 4.7 show the variation of the mean temperature at the collector output as a function of the intensity of solar radiation for the six models studied. There is a linear increase in all temperatures. According to Figures 4.6 and 4.7, the temperatures at the collector output of 6 ranges and the collector of 0.07 fin heights are high compared to other models, therefore, the figures above confirm the proportionality between the temperature at the collector output and its exchange face.

As expected, temperature values and flow are gradually increased until they reach a maximum value at noon, and then decrease later at the end of the day. It should be noted that the maximum values of the average temperature at the collector output reach 394.56 and 404.95 respectively for the greatest height 0.07 and for the case of 2 rows.

Average temperature evolution at output as a function of input velocity

The results were taken for the following input parameters for each model:

- A solar intensity of 618 W/m2.
- An ambient temperature of 298 K.

a. For the three different number of rows

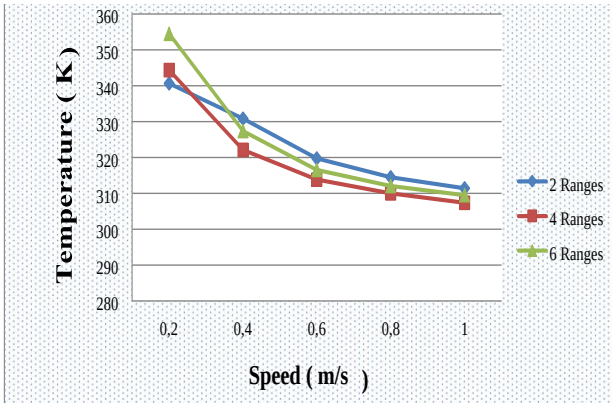

Figure 4.8: Evolution of the average temperature at the exit as a function of the speed of entry for the three different numbers of rows studied.

b. For the three different fin heights

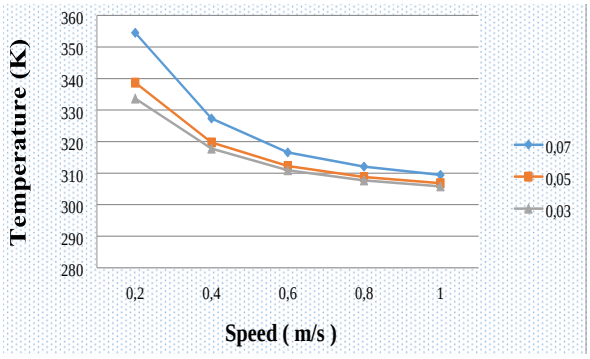

Figure 4. 9: Evolution of the average temperature at the exit as a function of the entry speed for the three different fin heights studied.

Figures 4.8 and 4.9 show the evolution of the mean temperature at the outlet for different speeds at the inlet for the six models studied.

The figures above show that there is an inverse relationship between velocity and temperature, where each time air velocity entering the collector increases, the more the average temperature at the collector output is dominated.

CONCLUSION

The main objective of this "work is to improve the performance of a solar collector in the presence of an absorber equipped with longitudinal fins. This thesis consists of a numerical study of the thermal and dynamic behaviour of air in a solar collector. Therefore, in order to achieve the desired goal, ANSYS FLUENT code was used to perform a numerical simulation of convective flow and visualize the various phenomena affecting the flow.

For the success of this thesis and to put our results in accuracy, a validation work of our numerical model was carried out by comparing them with experimental results. A good agreement was reached between them.

In this study, we proposed six solar collector models in total, three different number of rows and three different heights of fins. The thermos convective structure and dynamic behaviour of the flow were also analysed and interpreted for different values of solar radiation and air velocity at the inlet of the collector. This allowed us to draw multiple conclusions.

The increase in the number of rows plays a very important role in the thermal structure of the air flow, it significantly increases the absorber temperature and the air temperature at the outlet of the collector [19].

The increase in temperature at the solar collector outlet lays the radiative flux capture section and therefore increases proportionally with the increase of this section. The air temperature through the collector decreases with increasing air velocity at the chimney inlet. A very significant increase in the temperature of the collector absorber related to the increase in the height of the fins.

In short, given our study, for a good result of a solar collector in the presence of an absorber equipped with longitudinal fins, the collector which has a large number of rows and a fin height exactly the same as the height of the surface core presents the optimal collector".

REFERENCES

[1] Sharma, S.P. and Saha, S.N. (2017) Thermohydraulic Performance of Double Flow Solar Air Heater with Corrugated Absorber. International Journal of Energy and Power Engineering, 11, 779-785.

[2] Kalash, A.R., Shijer, S.S. and Habeeb, L.J. (2020) Thermal Performance Improvement of Double Pass Solar Air Heater. Journal of Mechanical Engineering Research and Developments, 43, 355-372.

[3] Ozgen, F., Esen, M. and Esen, H. (2009) Experimental Investigation of Thermal Performance of a Double-

Flow Solar Air Heater Having Aluminium Cans. Renewable Energy, 34, 2391-2398. https://doi.org/10.1016/j.renene.2009.03.029

[4] González, S.M., Larsen, S.F., Hernández, A. and Lesino, G. (2014) Thermal Evaluation and Modeling of a Double-Pass Solar Collector for Air Heating. Energy Procedia, 57, 2275-2284. https://doi.org/10.1016/j.egypro.2014.10.235

[5] Adil, M., Ibrahim, O., Hussein, Z. and Waleed, K. (2015) Experimental Investigation of SAHs Solar Dryers with Zigzag Aluminum Cans. International Journal of Energy and Power Engineering, 4, 240-247.https://doi.org/10.11648/j.ijepe.20150405.11

[6] Korti, A.I.N. (2015) Numerical 3-D Heat Flow Simulations on Double-Pass Solar Collector with and without Porous Media. Journal of Thermal Engineering, 1, 10-23. https://doi.org/10.18186/jte.86295

[7] Nowzari, R., Aldabbagh, L.B.Y. and Mirzaei, N. (2011) Experimental Study on Double Pass Solar Air Heater with Mesh Layers as Absorber Plate. International Journal of Electronics, Mechanical and Mechatronics Engineering, 3, 673-682.

[8] Ho, C., Lin, C., Yang, T. and Chao, C. (2014) Recycle Effect on Device Performance of Wire Mesh Packed Double-Pass Solar Air Heaters. Energies, 7, 7568-7585. https://doi.org/10.3390/en7117568

[9] Aldabbagh, L.B.Y., Egelioglu, F. and Ilkan, M. (2010) Single and Double Pass Solar Air Heaters with Wire Mesh as Packing Bed. Solar Energy, 35, 3783-3787 https://doi.org/10.1016/j.energy.2010.05.028

[10] Ramani, B.M., Gupta, A. and Kumar, R. (2010) Performance of a Double Pass Solar Air Collector. Solar Energy, 84, 1929-1937. https://doi.org/10.1016/j.solener.2010.07.007

[11] Omojaro, A.P. and Aldabbagh, L.B.Y. (2010) Experimental Performance of Single and Double Pass Solar Air Heater with Fins and Steel Wire Mesh Absorber. Applied Energy, 87, 3759-3765. https://doi.org/10.1016/j.apenergy.2010.06.020

[12] Maraba, G. (2012) An Experimental Study on Enhancement of Heat Transfer in a Solar Air Heater Collector by Using Porous Medium. October 2012 Izmir, Department of Mechanical Engineering, Iztech. A Thesis Submitted to the Graduate School of Engineering and Sciences of İzmir Institute of Technology.